Journal of Applied Veterinary Sciences, 9 (1): 13 – 21 (January, 2024).
ISSN: Online: 2090-3308, Print: 1687-4072
Journal homepage : https://javs.journals.ekb.eg

Ultrasonographic Anatomy, Electrophysiological and Histological Studies on Sciatic Nerve in Dog

Mona M. Khaled[1], Asmaa M. Ibrahium[1], Ahmed I. Abdelgalil[2], Mohamed A. El-Saied[3], Nagy Abouquerin[4] and Samah H. El-Bably[1]

[1]Department of Anatomy & Embryology, Faculty of Veterinary Medicine, Cairo University, Egypt
[2]Department of Surgery, Anaesthesiology, and Radiology, Faculty of Veterinary Medicine, Cairo University, Egypt
[3]Department of Pathology, Faculty of Veterinary Medicine, Cairo University, Egypt
[4]Department of Physiology, Faculty of Medicine, Ain Shams University, Egypt
***Corresponding Author:** Mona M. Khaled, **E-Mail:** mona.mohamed@vet.cu.edu.eg

ABSTRACT

The sciatic nerve is the major mixed nerve of the canine hind limb. It supplies most of the hind limb musculature. Sciatic nerve morphology and ultrasound guide surgeons and clinicians who contribute to the neurological examination of the sciatic nerve. So, the current study aimed to provide a fully descriptive ultrasonographic anatomy of the normal sciatic nerve in dogs and to set the motor conduction reference values of this nerve. Ultrasonography and neurography were applied to five adult healthy male dogs; two of them were euthanized for morphological and histological studies to describe the origin, branches, and innervated muscles of the sciatic nerve. The sciatic nerve originates from the ventral branches of the L6, L7, and S1 spinal nerves, splitting into muscular and sural branches, and is terminated by the perineal and tibial nerves. The normal sciatic nerve appears to have a hypoechoic core surrounded by hyperechoic bundles. The mean of the estimated electrophysiological parameters of the tibial and common fibular nerves was 2.20, 4.88, 20.08, 67, and 2.50, 7.78, 14.82, and 72.80 for the duration, latency, amplitude, and conduction velocity, respectively. Histological evaluation of the sciatic nerve revealed several nerve fasciculi surrounded by an epineural connective tissue sheath. The study provides a professional descriptive evaluation of the ultrasonographic anatomy of the sciatic nerve from its origin until divergence at the distal femur, which facilitates sciatic nerve evaluation for beginners and practitioners. The study also provides a full description of the neurographical and histological data of the normal sciatic nerve in dogs, which can be used as reference values for comparison with dogs that suffered sciatic nerve injuries.

Original Article:
DOI: HTTPS://DX.DOI.ORG/10.21608/JA 2023.232947.1267
Received : 03 September, 2023.
Accepted :25 October, 2023.
Published in January, 2024.

Keywords: Dogs, Electrophysiology, Histology, Sciatic nerve, Ultrasonographic anatomy.

J. Appl. Vet. Sci., 9(1): 13-21.

INTRODUCTION

Sciatic nerve is considered one of the main branches that arose from the lumbosacral plexus. The sciatic nerve is the largest peripheral nerve in the body, and it supplies most of the hind limb muscles **(Mahler and Adogwa, 2008; Khaled *et al.*, 2023).** Sciatic nerve anatomy was studied in dogs **(Echeverry *et al.*, 2010; Evans and De Lahunta, 2013; Sievert *et al.*, 2017),** cats **(Haro *et al.*, 2011; Haro *et al.*, 2012; Dayer *et al.*, 2017; El-Bably and Abdelgalil, 2018),** sheep **(Gojri *et al.*, 2022),** and laborator animals **(Asato *et al.*, 2000).**

Ultrasonography of the sciatic nerve was a safe and valuable diagnostic tool for evaluation of the nerve discontinuity, textural abnormalities, border irregularities, and neuroma formation without the need for general anesthesia. Sciatic ultrasonography also helps in locating the nerve during nerve block regional anaesthesia **(Martinoli *et al.*, 2002; Benigni *et al.*, 2007; Costa-Farré *et al.*, 2011; Marolf *et al.*, 2019; Micieli *et al.*, 2021; Toijala *et al.*, 2021).**

Electrophysiological examination is one of the major diagnostic procedures for evaluating the functional condition of the nerve and its electrical state **(Kimura, 2001; Cuddon, 2002).** It was

considered an important tool for the evaluation of different nerve disorders, including ischemic, inflammatory, traumatic, toxic, metabolic, and degenerative illnesses of the neuromuscular system, axonal neuropathy, and nerve tumours **(Platt, 2010).** The most commonly evaluated techniques in this field are electromyography (EMG) and nerve conduction velocity (NCV) values. NCS is considered the ideal and gold standard for the diagnosis of neuropathies **(Giza *et al.*, 2014).**

Peripheral nerve histopathological evaluation is considered the most common predictor of peripheral nerve injury and regeneration **(Vleggeert-Lankamp, 2007: Castro *et al.*, 2008).** Histological evaluation of the peripheral nerve injury and regeneration was the gold standard for evaluating the quality of nerve healing **(Geuna *et al.*, 2009).**

So, the current study aimed to provide fully detailed anatomical, sonographic, neurophysiological, and histological studies on the sciatic nerve along its course to set complete reference data for researchers and practitioners and provide a guide catalogue for surgeons dealing with any pathological cases related to this nerve.

MATERIALS AND METHODS

Ethical approval

This study was approved by the Institutional Animal Care and Use Committee at the Faculty of Veterinary Medicine, Cairo University, Egypt with number (Vet CU 01122022595).

Animals

The current study was conducted on five male Mongrel dogs with average weight (15-20 kg) and age (1-3 years). Ultrasonography and electrophysiology were done in all dogs. Two dogs of them were euthanized for histological and anatomical study.

Ultrasonographic study

The thigh region was clipped and shaved from the external angle of the ilium to the level of the popliteal fossa in both the right and left legs, and then acoustic coupling gel was applied. Sonographic imaging was performed using the Hitachi device Aloka F37 (Japan Medical Company, Tokyo, Japan) with an 8–10 MHz linear probe and colour Doppler. B-mode longitudinal and transverse scans were carried out first, then colour mode-activated. The course of the sciatic nerve and surrounding structures were scanned at four main levels (in the space between the caudal angle of the ilium and ischial tuberosity, just caudal to the greater trochanter, in the mid-thigh region, and at the popliteal fossa).

Electrophysiological studies

Under the effect of general anaesthesia using ylazine (1 mg/kg),, xylaject 2%® (Xyla-Ject® 2%, ADWIA Co., A.R.E.), and ketamine® (10 mg/kg) (Ketamar® 5%, Amoun Co., A.R.E.), dogs were placed in lateral recumbency with hind limbs extended at the stifle and abducted at the hip joints. Electrophysiology was performed using Trutrace (Czech Republic, Deymed); Traveller 4 Chanel system version 7.

Electrode placement and stimulation sites

Surface bipolar stimulation was used to deliver supramaximal stimulation. Active and reference surface electrodes were used for recording. The stimulating and recording electrodes were slightly coated with conductive gel (10-20 gel, USA, Weaver, and 565 Company). Another surface electrode was used as a ground electrode.

Motor nerve conduction studies were done for sciatic tibial nerve with an active surface electrode placed over the most prominent part of gastrocnemius muscle, and sciatic peroneal nerve with the electrode placed over the most prominent part of tibialis cranialis muscle and the reference electrode 2-3 cm distal to the active electrode in both.

Motor responses were obtained by delivering supramaximal stimulus at two stimulation sites. Proximal stimulation was done just caudal to the greater trochanter, and the distal stimulation site was about 5-7 cm distal to the site of proximal stimulus on the lateral aspect of the thigh region. The distance in between was measured to calculate the motor nerve conduction velocity.

Settings

Monitor time was set at 200 milliseconds (ms), stimulus duration at 0.2 msec, stimulus rate at 1 Hz (Hz), low-frequency filter at 20 Hz, and high-frequency filter at 3 kilohertz (kHz). The analysis time is 50 ms for motor studies. Also, initial sensitivity was 2 millivolts (mV) for motor nerve conduction and then increased or decreased according to the recorded response.

Measurements

Distal latency (DL): The time from the stimulus to the initial CMAPs deflection from baseline measured in milliseconds.

Duration: from the initial deflection from the baseline to the first baseline crossing measured in milliseconds.

Amplitude: measured from the baseline to the negative peak in mV.

Conduction velocity (CV): a measure of the speed of the fast-conducting axons and measured by this equation:

Distance between distal and proximal stimulation
Proximal latency – Distal latency

Anatomical investigation

Anatomical studies were done on two dogs after euthanasia with thiopental sodium (1 g) and pharcopental® (Thiopental®, EPICO, A.R.E.) intravenously. One of them was cannulated through the common carotid artery, formalised with formalin solution, and left for 3 days. After that, he was injected with saline solution (0.9%), then red latex neoprene, and left for 2–3 days before dissection. The second was dissected fresh, and one limb was dissected in situ to demonstrate the normal distribution of the nerve from its origin. Cross sections were applied throughout one fresh frozen limb by using a bone saw at two levels; one level was applied at the head of the femur and the other one at the mid-thigh region, correlated with sonographic scans.

Histological investigation

Histological samples were taken from the sciatic nerve of the freshly euthanized animal. Samples were preserved in neutral buffered formalin then processed, sectioned by microtome, and finally stained with hematoxylin-Eosin stain examined using an Olympus BX43 microscope connected with an Olympus digital camera (Olympus, Tokyo, Japan).

Statistical analysis

Data were summarized in tables as means and standard errors using Excel Microsoft Office 365.

RESULTS

Ultrasonographic anatomical investigations

The anatomical and ultrasonographic studies of the sciatic nerve were done at the same levels. There were three major bony structures, and four anatomical landmarks facilitated the ultrasonographic anatomical study.

First landmark

At the level between the caudal angle of the ilium and ischial tuberosity, present in the gluteal region, where the sciatic nerve trunk originated from the ventral branches of the L6, L7, and S1 spinal nerves. It traced the medial surface of the ilium as it passed between the deep gluteal muscle, middle gluteal, and piriform muscles. The sagittal scan revealed a hypoechoic core between two parallel hyperechoic lines (anechoic tubular structures) in between the hyperechoic iliac and ischial bones, while the transverse scan revealed three asymmetrical anechoic circular structures with thin hyperechoic margins (Fig. 1).

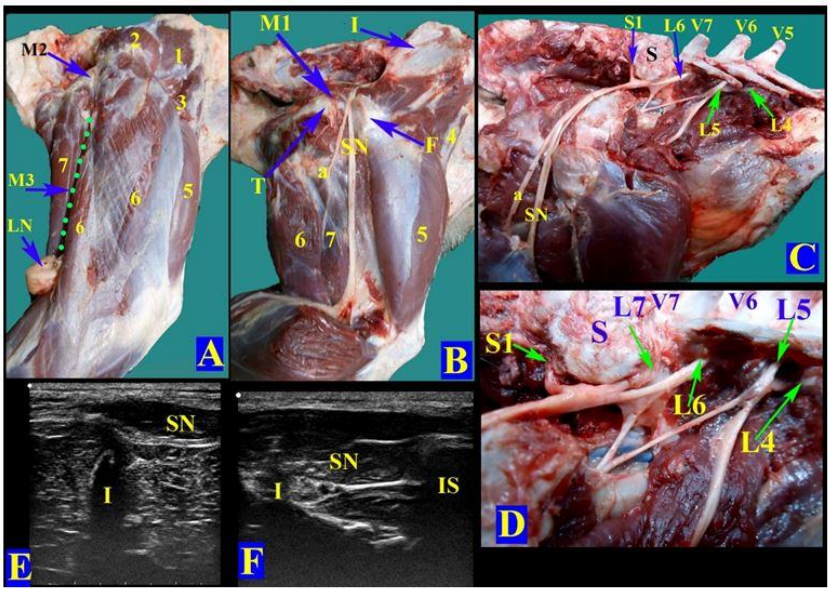

Fig. 1: A photograph showing lateral muscles of the hip region and origin of the sciatic nerve (Right side). A- Right lateral muscles of the hip and thigh regions, B- Course of the sciatic nerve (Reflected biceps femoris M), C & D- Origin of the lumbosacral plexus, E- Longitudinal scan of sciatic nerve, F- Transverse scan of sciatic Nerve at its origin. 1-middle gluteal M., 2- Superficial gluteal M., 3- Tensor faciae latae M., 4- Sartorius M., 5- Vastus lateralis M., 6- Biceps femoris M., 7-Semitendinosus muscle, SN-Sciatic nerve, a- Rami musculares, L.N-Popliteal lymph node, I- Ilium, IS- Ischium, T- Ischiatic tuberosity, F- Greater trochanter of femur, S- Sacrum, V5- Fifth lumbar vertebra, V6- Sixth lumbar vertebra, V7- Seven lumbar vertebra, S1- First sacral N., L4- Fourth lumbar N., L5- Fifth lumbar N., L6- Sixth lumbar N., L7- Seven lumbar N., M1- First anatomical landmark , M2- Second anatomical landmark, M3- Third anatomical landmark (Palpable space).

Second landmark

At the proximal aspect of the thigh, just caudal to the greater trochanter The sciatic nerve passed medial to the greater trochanter of the femur and sacrotuberal ligament, accompanied by caudal gluteal vessels, and deep to the biceps femoris muscle. A sagittal scan revealed the sciatic nerve appeared as two echogenic lines with an anechoic core just above the caudal gluteal artery, which appeared as a red line using the colour Doppler mode. The cross-section applied at the head of the femur showed the sciatic nerve was a white oval structure interlocated between the biceps femoris M. and semitendinosus M., caudal to the femur. A transverse scan revealed that the sciatic nerve appeared as two asymmetrical circular hypoechoic structures with a hyperechoic rim caudal to the hyperechoic greater trochanter (Figs. 2 and 3).

Third landmark

At the palpable space between biceps femoris and semitendinosus muscle, where the sciatic nerve coursed obliquely in between biceps and semitendinosus muscle in association with small abductor cruris caudalis muscle, where it sent four branches to them (rami musculares), then it became on succession on semimembranosus and adductor muscles. At the midshaft of the femur, transverse and sagittal scans were done in the palpable space between the biceps femoris and semitendinosus. In a longitudinal scan, the nerve appeared as a hypoechoic core structure surrounded by two hyperechoic lines sandwiched between hypoechoic biceps and semitendinosus muscles. A transverse scan revealed that the sciatic nerve appeared as two asymmetrical circular hypoechoic structures with a hyperechoic rim between the heterogenous hypoechoic muscles (Figs. 2 and 3).

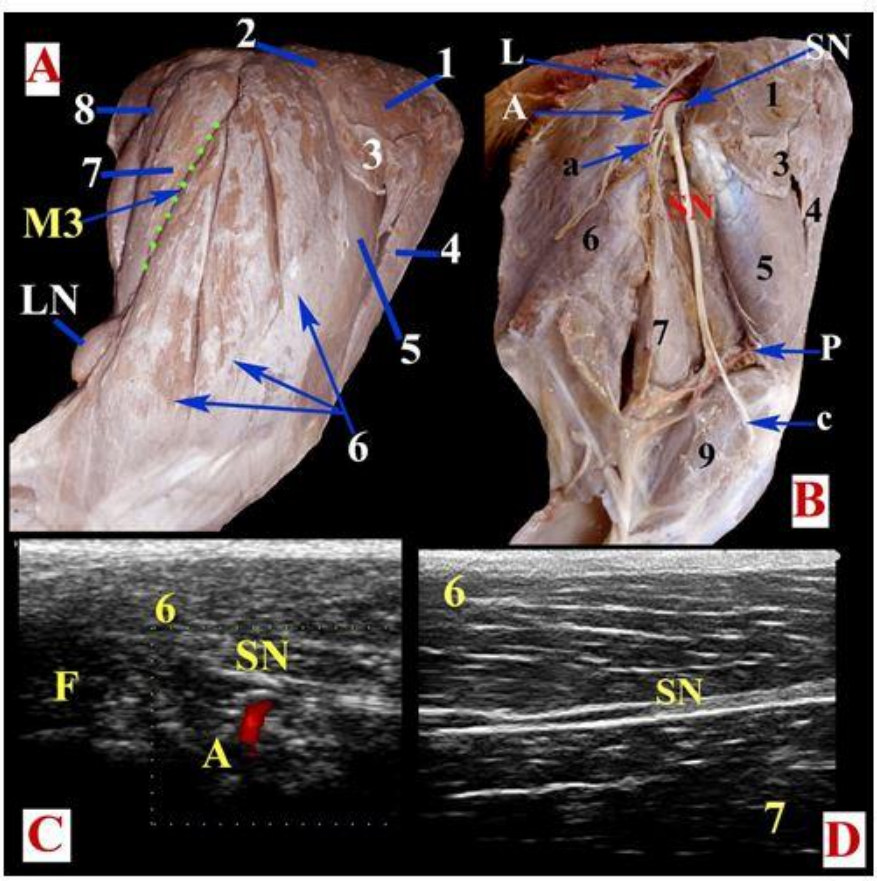

Fig. 2: A photograph showing lateral muscles of the thigh region (Left side). A- Left lateral muscles of the thigh region, B- Course of the sciatic nerve (Reflected biceps femoris M), C- Longitudinal scan at proximal thigh region, D- Longitudinal scan at middle thigh region 1-middle gluteal M., 2- Superficial gluteal M., 3-- Tensor faciae latae M., 4- Sartorius M., 5- Vastus lateralis M., 6- Biceps femoris M., 7-Semitendinosus muscle, 8-Semimembranosus M., 9- Gastrocnemius (Lateral head), SN-Sciatic nerve, a- Rami musculares, , c- common peroneal nerve, A-Caudal gluteal artery, P- Popliteal artery, LN- popliteal L.N, L- Sacrotuberal ligament, M3-Third anatomical mark (Palpable space), F- femur bone.

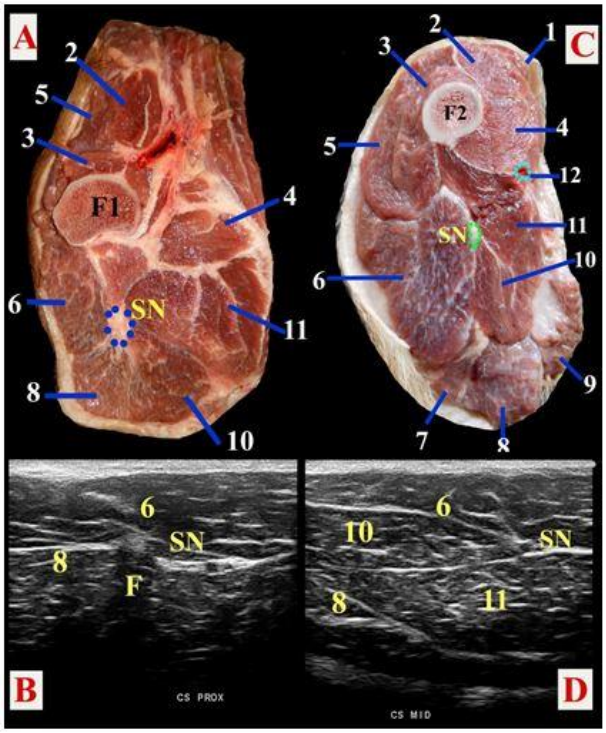

Fig. 3: A photograph showing the course of sciatic nerve in thigh region. A- Cross section at the Proximal-thigh region, B- Transverse scan at proximal- thigh, C- Cross section at the mid-thigh region and D-Transverse scan at mid- thigh. 1-Sartorius M., 2-Rectus femoris M., 3-Vastus intermediate M., 4-Vastus medialis M., 5-Vastus lateralis M., 6-Biceps femoris M., 7-Abductor cruralis M., 8-Semitendinosus M., 9- Gracilis M., 10-semimembranosus M., 11-Adductor M., 12-Femoral artery, F- Femur, SN-sciatic nerve.

Fourth landmark

At the distal third of the thigh region dorsal to the popliteal fossa, the sciatic nerve terminates into two main branches, the common peroneal (fibular) and tibial nerves, in association with the caudal femoral artery and popliteal blood vessels. Caudal cutaneous sural nerves, where three fine branches arose from the caudal border of the sciatic nerve, ran distally beneath the biceps femoris muscle to become in close contact with the gastrocnemius (plantar surface), supplying skin at the caudal aspect of the crus region. A sagittal scan showed the division of the sciatic nerve into two nerves with the same ultrasonographic characteristics as the sciatic nerve (hypoechoic structure surrounded by two echogenic lines), but these nerves appeared smaller in diameter. At the bifurcation of the sciatic nerve, the caudal femoral artery appeared as an anechoic circular structure in B mode and appeared as a red spherical structure in Doppler mode (Fig 4).

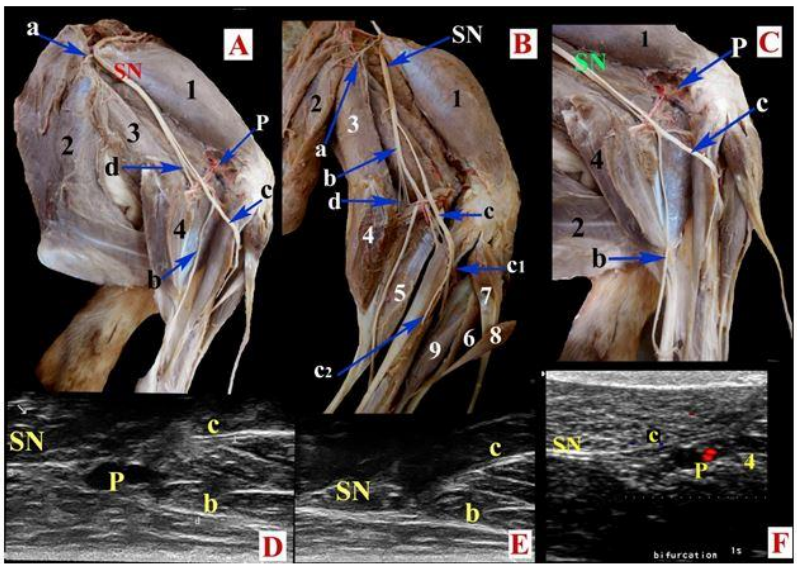

Fig.4: A photograph showing the sciatic nerve at the thigh and crus regions (Left side). A-Course of sciatic at popliteal fossa, B & C-Division of sciatic at popliteal fossa, D, E & F Longitudinal scan at thigh distal region. 1-Vastus lateralis M., 2- Biceps femoris M. (reflected caudally), 3-Semitendinosus M., 4-Gastrocnemius M.(lateral head, reflected caudally), 5- Superficial digital flexor M. , 6-Cranial tibial M., 7-Long fibular M., 8-Lateral digital extensor M., 9 -Long digital extensor M., SN-Sciatic nerve, a- Rami musculares, b-tibial nerve, c- common peroneal nerve, d-Caudal cutaneous sural Ns., c1- Deep branch of common peroneal N., c2- Superficial branch of common peroneal N., P- Distal caudal femoral artery.

Histological investigation

Sciatic nerve revealed nerve bundles encircled by connective tissue perineurium. In the bundles, nerve fibers were held together by delicate connective tissue called endoneurium. Each fiber was formed of faint acidophilic axons surrounded by a myelin sheath (Fig.5).

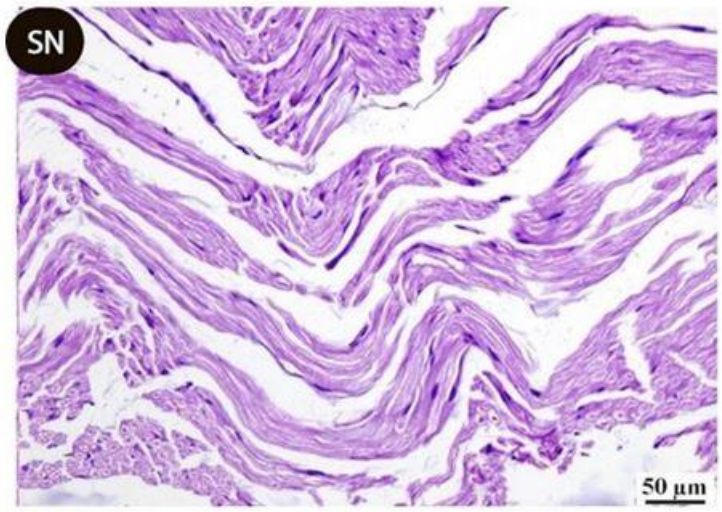

Fig.5: Histological section of sciatic nerve showed normal intact axons of the sciatic nerve that oriented longitudinally enclosed with myelin sheaths (H&E)

Electrophysiological study

The measurements of motor nerve conduction velocity (MNCV) of both tibial and peroneal nerves (terminal branches of the sciatic nerve) were summarized in Table 1 and Table 2. Differences in values of conduction velocity (CV) and amplitude between five dogs were related to differences in age and average body weight, whose ranges were 1-3 years and 15-20 kg, respectively (Fig 6).

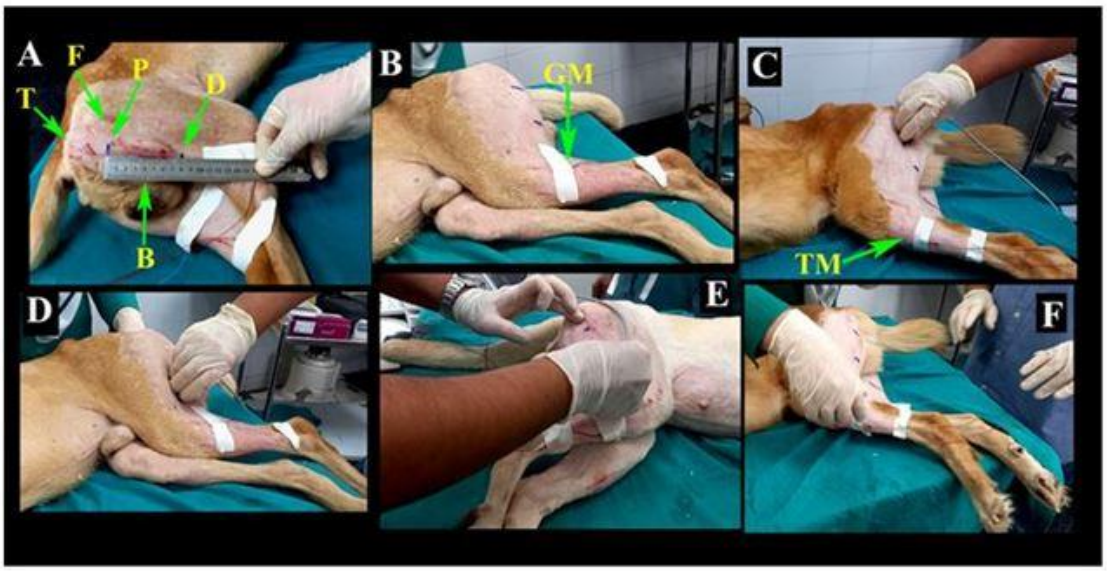

Fig. 6: Showing the procedure of measurements of Motor nerve conductivity (Tibial and peroneal nerve conduction). F- Greater trochanter of femur, T- Ischiatic tuberosity, P- proximal stimulus, D- Distal stimulus, B- The distance between the proximal stimulus and distal one (palpable space), GM- Gastrocnemius M., TM- Cranial tibial M.

Table 1. Measurements of electro-neurology of left tibial nerve.

	Tibial Nerve			
	DL	Duration	amplitude	CV
DOG 1	2.1	3.6	21.9	60
DOG 2	2.1	5.5	16.3	48
DOG 3	2.6	4.2	19.3	83
DOG 4	2.2	4.7	28.7	71
DOG 5	2.0	6.4	14.2	73
Mean ± SE	2.20 ± 0.10	4.88 ± 0.49	20.08 ± 2.52	67 ± 5.99

Table 2. Measurements of electro-neurology of left peroneal nerve.

	Common Peroneal Nerve			
	DL	Duration	amplitude	CV
DOG 1	2.5	6.8	14.3	65
DOG 2	2.9	10.0	11.8	68
DOG 3	2.7	7.0	13.1	75
DOG 4	2.2	8.5	17.9	67
DOG 5	2.2	6.6	17.0	89
Mean ± SE	2.50 ± 0.12	7.78 ± 0.58	14.82 ± 1.03	72.80 ± 3.92

DISCUSSION

Ultrasonographic anatomy and electrophysiology were easily and accurately studied based on palpable bony landmarks. Anatomical studies revealed that the sciatic nerve originated from the ventral branches of the L6, L7, and S1 spinal nerves, and that was similar to findings reported by Ueyama **(1978).** On the contrary, Bennett **(1976) and Sievert *et al.*, (2017)** reported that S2 was incorporated into the origin. **Bennett (1976)** estimated that the origin of sciatic nerves in dogs (L6, L7, SI, and S2) was similar to those of cats, with fine differences in the contribution of lumbar and sacral nerves in the formation of tibial and fibular nerves.

The sciatic nerve exited the pelvis through the greater ischiatic foramen and continued medial to greater trochanter of the femur associated with caudal gluteal vessels; it entered the thigh region deep into the biceps femoris muscle and also terminated into the tibial and common peroneal nerves. These findings were in the same vein as those of **Mahler and Adogwa (2008); Campoy *et al.*, (2010); Echeverry *et al.*, (2010) and Sievert *et al.*, (2017)**.

Our study showed that ultrasonographic scanning of the sciatic nerve could be studied in four different regions, while **Benigni *et al.*, (2007) and Costa-Farré *et al.*, (2011)** reported their findings only in three regions. Sagittal and transverse scans were feasible at all levels. Ultrasonographic evaluation of the sciatic nerve origin at the sacroiliac articulation couldn't be done as it was covered completely by the ilium, which reflects all ultrasounds. In the current study, the sciatic nerve along its course appeared as a hypoechogenic structure surrounded by a hyperechogenic rim, and that result was in correlation with **Campoy *et al.*, (2010); Echeverry *et al.*, (2010)**. The hypoechoic portions of the sciatic nerve are likely to represent the neuronal fascicles, while the hyperechoic rim is likely to represent the epineurium **(Silvestri *et al.*, 1995).**

The sciatic nerve in the space between the ilium and ischial tuberosity appeared as three hypoechoic circles surrounded by a thin hyperechoic rim, which represent the ramus proximalis, peroneal, and tibial nerves. Colour Doppler ultrasonographic evaluation of the caudal gluteal vessels facilitates differentiation between them and the sciatic nerve at this level. **(Benigni *et al.*, 2007)** reported that at the level of the ischium, when there was uncertainty between the nerve and the caudal gluteal vessels, colour flow Doppler should be applied.

This study found that the sciatic nerve appeared as two hypoechoic structures along the thigh region until bifurcation. The larger component represents the tibial nerve, while the smaller one represents the common peroneal nerve, and these findings were in the same line with **Costa-Farré *et al.*, (2011)** who reported that the sciatic nerve appeared as regular bi-tubular hypoechoic bands surrounded by a thin hyperechoic rim, representing the larger tibial and smaller fibular nerves in the sagittal and transverse scans of the mid-thigh region. The echotexture of the sciatic nerve in our study resembled that described by **Hudson *et al.*, (1996)** and **Benigni *et al.*, (2007)**.

The longitudinal scan at the popliteal fossa revealed termination of sciatic nerve into tibial and fibular nerves that were distinguished as two hyperechoic lines with a hypoechoic core closely adjacent to anechoic circular structure related to the caudal femoral artery, in accordance with **Benigni *et al.*, (2007)** in dogs and **Haro *et al.*, (2011)** in cats. Sciatic nerve ultrasonography is superior to MRI and other diagnostic modalities for nerve evaluation as it enables changes in the nerve direction by changing the probe orientation to follow the nerve and also provides higher resolution than other diagnostic modalities.

Classically, the nerve trunk appeared under a light microscope as nerve bundles surrounded by epineurium connective tissue. Each individual

fasciculi (nerve bundle) is enclosed by a perineurium, which in turn enclosed the endoneurium, or intrafascicular connective tissue around individual nerve fibres, which was in agreement with the study proved by **Geuna *et al.*, (2009).** Each individual nerve fibre appeared as several acidophilic axons by H&E stain surrounded by its myelin sheath, as documented by **Chato-Astrain *et al.*, (2022).**

In the present study, electrophysiologic testing was conducted on the normal sciatic nerve in dogs by estimating the nerve conduction studies NCS values of both tibial and peroneal nerves to serve as guide data that can be used in the investigation of any abnormal disorders related to sciatic nerve. The current study revealed that the mean conduction velocity (MCV) of the tibial and peroneal nerves were 67±5.99 and 72.80±3.92 respectively. **Walker *et al.*, (1979)** It was reported that the MCV of the tibial and peroneal nerves were 68.2±1.4 and 79.8±1.8 (m/s ± SD), respectively, which was nearly similar to the values estimated by our study. Electrophysiological studies of the sciatic nerve play a potent and great role in determining alteration in function and many nerve neuropathies using motor and sensory studies **(Abraham *et al.*, 2003; De Lahunta *et al.*, 2009; Mortari *et al.*, 2018 ; Kim *et al.*, 2019).**

CONCLUSION

The study provides a professional descriptive evaluation of the ultrasonographic anatomy of the sciatic nerve from its origin until bifurcation at the distal femur, which facilitates sciatic nerve evaluation for beginners and practitioners. The study also provides a full description of the neurographical and histological data of the normal sciatic nerve in dogs, which can be used as reference values for comparison with dogs that suffered sciatic nerve injuries.

Funding

This study was funded by SDFT according to the agreement between Springer Nature, EKB, and Cairo University.

Data availability

All data collected or analyzed during this study are included in this published review article.

Conflict of interests

The authors declare no potential conflict of interest.

REFERENCES

ABRAHAM, L., MITTEN, R., BECK, C., CHARLES, J., and HOLLOWAY, S., 2003. Diagnosis of sciatic nerve tumour in two dogs by electromyography and magnetic resonance imaging. *A*ustralian veterinary journal, 81(1-2), 42-46. https://doi.org/10.1111/j.1751-0813.2003.tb11421.x

ASATO, F., BUTLER, M., BLOMBERG, H., and GORDH, T., 2000. Variation in rat sciatic nerve anatomy: implications for a rat model of neuropathic pain. Journal of the Peripheral Nervous System, 5(1), 19-21. https://doi.org/10.1046/j.1529-8027.2000.00155.x

BENIGNI, L., CORR, S. A., and LAMB, C. R., 2007. Ultrasonographic assessment of the canine sciatic nerve. Veterinary Radiology & Ultrasound, 48(5), 428-433. https://doi.org/10.1111/j.1740-8261.2007.00273.x

BENNETT, D. 1976. An anatomical and histological study of the sciatic nerve, relating to peripheral nerve injuries in the dog and cat. Journal of Small Animal Practice, 17(6), 379-386. https://doi.org/10.1111/j.1748-5827.1976.tb06974.x

CAMPOY, L., BEZUIDENHOUT, A. J., GLEED, R. D., MARTIN-FLORES, M., RAW, R. M., SANTARE, C. L., JAY, A. R., and WANG, A. L., 2010. Ultrasound-guided approach for axillary brachial plexus, femoral nerve, and sciatic nerve blocks in dogs. Veterinary anaesthesia and analgesia, 37(2), 144-153. https://doi.org/10.1111/j.1467-2995.2009.00518.x

CASTRO, J., NEGREDO, P., and AVENDAÑO, C., 2008. Fiber composition of the rat sciatic nerve and its modification during regeneration through a sieve electrode. Brain research, 1190, 65-77. https://doi.org/10.1016/j.brainres.2007.11.028

CHATO-ASTRAIN, J., GARCÍA-GARCÍA, O. D., CAMPOS, F., SÁNCHEZ-PORRAS, D., and CARRIEL, V., 2022. Basic Nerve Histology and Histological Analyses Following Peripheral Nerve Repair and Regeneration. Peripheral Nerve Tissue Engineering and Regeneration, 151. https://doi.org/10.1016/j.bbrc.2020.04.094

COSTA-FARRÉ, C., BLANCH, X. S., CRUZ, J. I., and FRANCH, J., 2011. Ultrasound guidance for the performance of sciatic and saphenous nerve blocks in dogs. The Veterinary Journal, 187(2), 221-224. https://doi.org/10.1016/j.tvjl.2009.10.016

CUDDON, P. A. 2002. Electrophysiology in neuromuscular disease. Veterinary Clinics: Small Animal Practice, 32(1), 31-62. https://doi.org/10.1016/S0195-5616(03)00079-2

DAYER, T., ROHRBACH, H., FORTERRE, S., STOFFEL, M. H., and FORTERRE, F., 2017. Investigation of sciatic nerve surgical anatomy in dogs and cats: a comparative cadaveric study. International Journal of Veterinary Science, 6(3), 131-135. http://dx.doi.org/10.7892/boris.108853

DE LAHUNTA, A., GLASS, E., and KENT, M., 2009. Lower motor neuron: spinal nerve, general somatic efferent system. Veterinary neuroanatomy and clinical neurology, 3, 119-120. https://doi.org/10.1016/j.mehy.2007.09.011

ECHEVERRY, D. F., GIL, F., LAREDO, F., AYALA, M. D., BELDA, E., SOLER, M., and AGUT, A., 2010. Ultrasound-guided block of the sciatic and femoral nerves in dogs: a descriptive study. The Veterinary Journal, 186(2), 210-215. https://doi.org/10.1016/j.tvjl.2009.08.005

EL-BABLY, S., and ABDELGALIL, A., 2018. Ultrasonographic anatomy of the equine carpal region (Equus caballus). International Journal of Veterinary Science, 7(1), 44-49.

EVANS, H. E., and DE LAHUNTA, A., 2013. Miller's anatomy of the dog-E-Book. Elsevier health sciences.

GEUNA, S., RAIMONDO, S., RONCHI, G., DI SCIPIO, F., TOS, P., CZAJA, K., and FORNARO, M., 2009. Histology of the peripheral nerve and changes occurring during nerve regeneration. International review of neurobiology, 87, 27-46. https://doi.org/10.1016/S0074-7742(09)87003-7

GIZA, E., NICPON, J., and WRZOSEK, M., 2014. Clinical and Electrodiagnostic Findings in A Cohort of 61 Dogs with Peripheral Nervous System Diseases-A Retrospective Study. Pakistan Veterinary Journal, 34(2).

GOJRI, B. A., PARRAH, J.-U.-D., DAR, M.-U.-D., AHMAD, R. A., RESHI, P. A., and FAROOQ, U. B., 2022. Gross and sonographic anatomy of sciatic nerve in fecB Sheep. *SKUAST* Journal of Research, 242), 242-247. http://dx.doi.org/10.5958/2349-297X.2022.00044.7

HARO, P., GIL, F., LAREDO, F., AYALA, M. D., BELDA, E., SOLER, M., and AGUT, A., 2011. Ultrasonographic study of the feline sciatic nerve. Journal of feline medicine and surgery, 13(4), 259-266. https://doi.org/10.1016/j.jfms.2010.12.004

HARO, P., LAREDO, F., GIL, F., BELDA, E., AYALA, M. D., SOLER, M., and AGUT, A., 2012. Ultrasound-guided block of the feline sciatic nerve. Journal of feline medicine and surgery, 14(8), 545-552. https://doi.org/10.1177/1098612X12443749

HUDSON, J., STEISS, J., BRAUND, K., and TOIVIO-KINNUCAN, M., 1996. Ultrasonography of peripheral nerves during Wallerian degeneration and regeneration following transection. Veterinary Radiology & Ultrasound, 37(4), 302-312. https://doi.org/10.1016/j.jneumeth.2010.02.023

KHALED, M. M., IBRAHIUM, A. M., ABDELGALIL, A. I., EL-SAIED, M. A., and EL-BABLY, S. H., 2023. Regenerative Strategies in Treatment of Peripheral Nerve Injuries in Different Animal Models. Tissue Engineering and Regenerative Medicine, 1-39. https://doi.org/10.1007/s13770-023-00559-4

KIM, S. Y., GEORGY, J. S., and IVANOV, Y. O., 2019. Clinical Nerve Function Studies and Imaging. In Academic Pain Medicine (pp. 105-110). Springer. https://doi.org/10.1007/978-3-030-18005-8

KIMURA, J. (2001). Principles and variation of nerve conduction studies. Electrodiagnosis in diseases of nerve *and* muscle: principles and practice. https://doi.org/10.1002/ana.410160402

MAHLER, S. P., and ADOGWA, A. O., 2008. Anatomical and experimental studies of brachial plexus, sciatic, and femoral nerve-location using peripheral nerve stimulation in the dog. Veterinary anaesthesia and analgesia, 35(1), 80-89. https://doi.org/10.1111/j.1467-2995.2007.00356.x

MAROLF, V., ROHRBACH, H., BOLEN, G., VAN WIJNSBERGHE, A.-S., and SANDERSEN, C.M., 2019. Sciatic nerve block in dogs: description and evaluation of a modified ultrasound-guided parasacral approach. Veterinary anaesthesia and analgesia, 46(1), 106-115. https://doi.org/10.1016/j.vaa.2018.10.003

MARTINOLI, C., BIANCHI, S., DAHMANE, M. H., PUGLIESE, F., BIANCHI-ZAMORANI, M., and VALLE, M., 2002. Ultrasound of tendons and nerves. European radiology, 12(1), 44-55. https://doi.org/10.1007/s00330-001-1161-9

MICIELI, F., CHIAVACCINI, L., MENNONNA, G., DELLA VALLE, G., PRISCO, F., MEOMARTINO, L., and VESCE, G., 2021. An ultrasound-guided subparaneural approach to the sciatic nerve in the dog: a cadaver study. Veterinary anaesthesia and analgesia, 48(1), 107-115. https://doi.org/10.1016/j.vaa.2020.06.008

MORTARI, A. C., QUITZAN, J. G., BRANDÃO, C. V. S., and RAHAL, S. C., 2018. Sciatic Nerve Injection Palsy in a Dog: Electrodiagnostic Testing and Microsurgical Treatment. Acta Scientiae Veterinariae, 46, 4. https://doi.org/10.22456/1679-9216.86738

PLATT, S. 2010. Small Animal Neurology: An Illustrated Text. Schlütersche.

SIEVERT, C., RICHTER, H., GASCHO, D., KIRCHER, P. R., and CARRERA, I., 2017. 3 Tesla magnetic resonance imaging study of the normal canine femoral and sciatic nerves. Veterinary Radiology & Ultrasound, 58(5), 598-606. https://doi.org/10.1111/vru.12511

SILVESTRI, E., MARTINOLI, C., DERCHI, L. E., BERTOLOTTO, M., CHIARAMONDIA, M., and ROSENBERG, I., 1995. Echotexture of peripheral nerves: correlation between US and histologic findings and criteria to differentiate tendons. Radiology, 197(1), 291-296. https://doi.org/10.1148/radiology.197.1.7568840

TOIJALA, T. M., CANAPP, D. A., and CANAPP, S. O., 2021. Ultrasonography Findings in the Proximal Sciatic Nerve and Deep Gluteal Muscles in 29 Dogs With Suspected Sciatic Neuritis. Frontiers in Veterinary Science, 8. https://doi.org/10.3389%2Ffvets.2021.704904

UEYAMA, T. 1978. The topography of root fibres within the sciatic nerve trunk of the dog. Journal of Anatomy, 127(Pt 2), 277.

VLEGGEERT-LANKAMP, C. L. 2007. The role of evaluation methods in the assessment of peripheral nerve regeneration through synthetic conduits: a systematic review. Journal of neurosurgery, 107(6), 1168-1189. https://doi.org/10.3171/JNS-07/12/1168

WALKER, T., REDDING, R., and BRAUND, K., 1979. Motor nerve conduction velocity and latency in the dog. American journal of veterinary research, 40(10), 1433-1439. PMID: 525865.

How to cite this article:
Mona M. Khaled, Asmaa M. Ibrahium, Ahmed I. Abdelgalil, Mohamed A. El-Saied, Nagy Abouquerin and Samah H. El-Bably, 2024. Ultrasonographic Anatomy, Electrophysiological and Histological Studies on Sciatic Nerve in Dog. Journal of Applied Veterinary Sciences, 9 (1): 13-21.
DOI:HTTPS://DX.DOI.ORG/10.21608/JAVS.2023.232947.1267